Silylones

DOI: 10.1002/anie.201308609

Experimental Charge Density Study of a Silylone**

Benedikt Niepötter, Regine Herbst-Irmer, Daniel Kratzert, Prinson P. Samuel, Kartik Chandra Mondal, Herbert W. Roesky, Paul Jerabek, Gernot Frenking,* and Dietmar Stalke**

In memory of Daniel Kost

Abstract: *An experimental and theoretical charge density study confirms the interpretation of $(cAAC)_2Si$ as a silylone to be valid. Two separated VSCCs present in the non-bonding region of the central silicon are indicative for two lone pairs. In the experiment, both the two crystallographically independent Si−C bond lengths and ellipticities vary notably. It is only the cyclohexyl derivative that shows significant differences in these values, both in the silylones and the germylones. Only by calculating increasing spheres of surrounding point charges we were able to recover the changes in the properties of the charge density distribution caused by weak intermolecular interactions. The nitrogen–carbene-carbon bond seems to have a significant double-bond character, indicating a singlet state for the carbene carbon, which is needed for donor acceptor bonding. Thus the sum of bond angles at the nitrogen atoms seems to be a reasonable estimate for singlet versus triplet state of cAACs.*

Although located in the same group in close proximity in the periodic table, species of low-valent carbon and silicon show colossal differences in their stability. Both are very interesting compounds because of for example their ability to activate small molecules, such as transition-metal complexes do. Coined after their carbon analogues known as the carbones, molecules containing a low-valent silicon atom in oxidation state zero with formally two lone pairs at the central silicon atom and stabilized by donor–acceptor bonds of, for example, N-heterocyclic carbenes (NHCs), are called silylones.[1] The term carbone was introduced by Frenking et al.[2] They concluded by calculations on different allenes that the deviation from the linear geometry could be rationalized by donor–acceptor bonds in lieu of double bonds.[3] Experimental evidence for this was provided by Bertrand et al.[4] and Fürstner et al.[5] Subsequently the bonding in these molecules was vigorously discussed.[6] An allene congener of silicon was long sought after. In 2003 Kira et al.[7] reported the first silaallene with a Si=Si=Si angle of 136.49°. Only one additional silaallene has been reported to date.[8] Calculations suggest that Kira's silaallene better should be described as a silylone.[1] This interpretation was explained with the shape of the HOMO and HOMO−1 and with extremely high first and second proton affinities.[1] In contrast, further calculations by Kosa et al. and Veszprémi et al. led to different conclusions.[9] Thus the case remains open to experiment, as it is obvious that various ligands attached to the central silicon atom provide the ultimate impact on the bonding situation. In 2009, calculations on various NHC-stabilized compounds $(NHC)_2Si$ showed that a silylone with two NHC ligands should experimentally be feasible.[1,6e] Recently we reported the first silylone $(cAAC)_2Si$ (**2**) stabilized by two cyclic alkyl amino carbenes (cAACs)[10] synthesized by reduction of the singlet silicondichloride biradical[11] (**1**; analogous to Scheme 1). The existence of a silicon(0) stabilized by two donor–acceptor bonds of the cAACs was confirmed by calculations[11a] and by the geometry of the cAACs from an independent atom model (IAM) based on diffraction experiments.[12] A second silylone was reported by Driess et al. recently.[13] Even though there are some reports on experimental charge density studies on low-valent silicon compounds, no experimental charge density study on a silylone has yet been reported.[14]

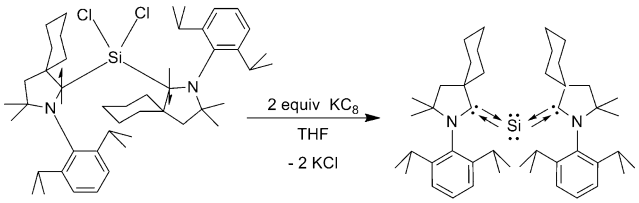

1 **2**

Scheme 1. Synthesis of silylone **2** from **1** upon KC_8 reduction.

Herein, we present the analysis of the bonding situation in **2** using experimental charge-density investigations. Based on a structure model refined against high-resolution data using

[*] B. Niepötter, Dr. R. Herbst-Irmer, Dr. D. Kratzert, Dr. P. P. Samuel, Dr. K. C. Mondal, Prof. Dr. H. W. Roesky, Prof. Dr. D. Stalke
Institut für Anorganische Chemie, Georg-August-Universität
Tammannstrasse 4, 37077 Göttingen (Germany)
E-mail: hroesky@gwdg.de
dstalke@chemie.uni-goettingen.de
P. Jerabek, Prof. Dr. G. Frenking
Fachbereich Chemie, Phillips-Universität
Hans-Meerwein-Strasse, 35032 Marburg (Germany)
E-mail: frenking@chemie.uni-marburg.de

[**] We thank the Fonds der Chemischen Industrie and the Danish National Research Foundation (DNRF93) funded Center for Materials Crystallography (CMC) for support. H.W.R. thanks the Deutsche Forschungsgemeinschaft (DFG RO 224/60-1) for financial support.

Supporting information for this article is available on the WWW under http://dx.doi.org/10.1002/anie.201308609.

the Hansen and Coppens multipole model,[15] the electron density (ED) distribution $\rho(r)$ was analyzed by topological analysis according to Bader's quantum theory of atoms in molecules (QTAIM).[16] This allows the characterization of bonds as well as the determination of atomic charges. An atomic basin is defined by the zero flux surfaces ($\nabla\rho(r)\,n(r)=0$). Integration of the ED in this basin gives the Bader charge. Bonds are characterized for example by looking at the properties along the bond path and at the (3,−1) critical points, the bond critical points (BCPs), where the ED along the bond path between two bonded atoms locally reaches its minimum.

A negative Laplacian $\nabla^2\rho(r_{BCP})$ shows local concentration of the ED. A negative Laplacian at the BCP accompanied by a high ED indicates the covalent character of a bond. On the other hand, a distinct positive Laplacian and low ED at the BCP are associated with closed-shell interactions. However, for very polar bonds, this categorization cannot be applied strictly, but remains a feasible way to compare bonds. Further information can be received from the eigenvalues (λ_i) of the Hessian matrix. The ellipticity $\varepsilon_{BCP}=\lambda_1/\lambda_2-1$ quantifies the deviation from a cylindrical shape, indicating for example a higher π-contribution. An additional indicator for the bond type is given by $\eta=|\lambda_1|/\lambda_3$. The value of η_{BCP} is less than unity for closed shell interactions and increases with increasing covalent character. It is also possible to obtain information about lone pairs by analyzing the Laplacian. (3,−3) critical points in the second derivative, so-called valence-shell charge concentrations (VSCCs) indicate bonding or non-bonding electrons, although they should not be taken as a one-to-one representation of a Lewis lone pair.[17] Additionally to the QTAIM analysis of the experimental electron distribution we did an analysis of the electron density gained from calculations. These values are given in each case in squared brackets (see Table 2).

Compound **2** crystallizes in the triclinic space group $P\bar{1}$ containing one molecule of **2** and half of a hexane molecule as co-crystallized solvent molecule in the asymmetric unit. The molecular graph of **2** shows the central silicon atom solely connected to two cAACs. The C1-Si1-C24 angle of 119.10(1)° confirms that the molecule is by no means linear. We found two distinct VSCCs of −2.82 and −2.80 e Å^{-5} in the non-bonding region of the central silicon atom in the position where one would expect the lone pairs of a potential silicon(0) atom (Figure 1 and Figure 2).[18] That they are not involved in any chemical bonding renders them potential lone-pair indicators.[19]

The integrated Bader charges are 1.44 [1.27] for Si1, −0.51 [−0.31] for C1, and −0.37 [−0.26]e for C24, respectively. In an earlier NBO analysis[11a] of a similar compound, we suggested one of the lone pairs at the silicon atom to be delocalized over a three-center π-bond with probability distributions of 40% at the silicon atom and 30% at each carbene carbon atom. This would lead to an expected Bader charge of 1.2e for silicon and −0.6e for each carbene carbon atom, matching reasonably with the experimental values.

As we showed recently, the geometry at the nitrogen atoms in the cAAC is an indicator for the bonding situation in $(cAAC)_2X$ (X = $SiCl_2$, Si, BH) species.[12] A deviation from the planar geometry at the nitrogen atom such as in the free carbene should be observed if the bond between the central atom and the carbene carbon is an electron-sharing bond. However, molecules with a cAAC-X donor–acceptor bond do not show any deviation from a planar N environment. This could be explained by the different electronic nature of the carbenes. To provide a donor–acceptor bond situation the carbene carbon atom needs to be in the singlet state, thus the carbene p orbital is vacant. This enables the lone pair of the nitrogen to donate electron density into this vacant orbital and the C–N bond shows more π-character. A delocalization into the vacant p-orbital is hampered if the carbene is in the triplet state. Thus the lone pair orbital of the nitrogen atom acquires higher s character and the geometry tends to be more pyramidal. Therefore, the sum of bond angles at the nitrogen atom can be taken as a rough measure to distinguish a singlet from a triplet state even in IAM structures.

In **2** we found an almost ideally C_{3h} symmetric Laplacian distribution around both nitrogen atoms (Figure 3). The ED and the Laplacian at the BCP in the bonds between the nitrogen atoms (N1, N2) and the carbene atoms (C1, C24) in both are higher in absolute value than at the other BCPs and only they show significant ellipticities ε (Table 1).[20] Thus the

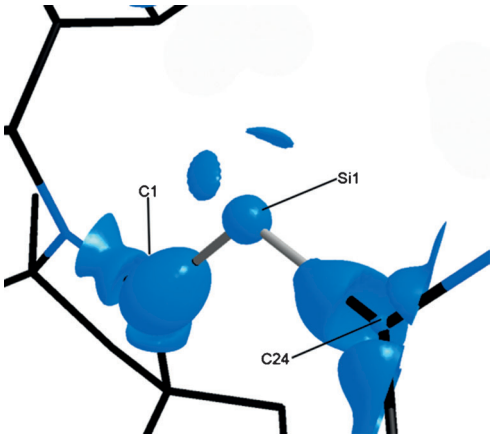

Figure 1. Laplacian distribution at the silicon atom in **2** at an isosurface level of −2.5 e Å^{-5}.

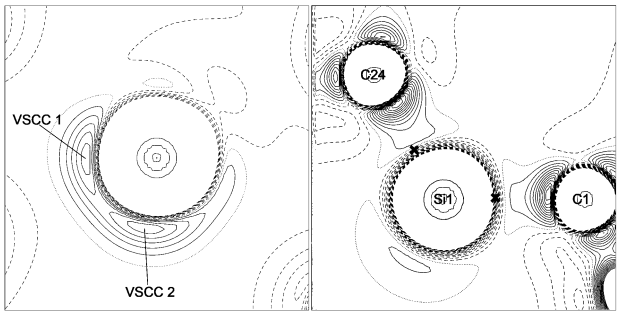

Figure 2. Laplacian distribution orthogonal to the C1–C24 vector (left) and in the C1-Si1-C24 plane (right). Contour lines are drawn at ±0.5, 1.0, 1.5, ... e Å^{-5} (left) and ±2, 4, 6, ... e Å^{-5} (right) interval level. Solid line: charge concentration, dashed line: charge depletion; the BCPs are depicted as black crosses.

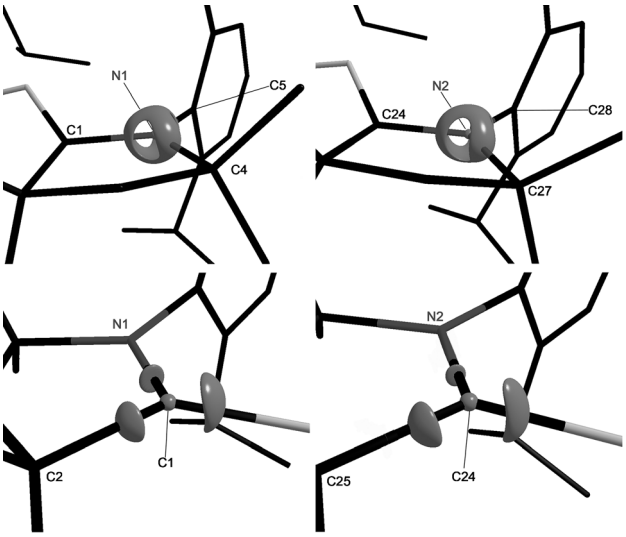

Figure 3. Laplacian distribution at N1 (top left) and N2 (top right) atoms of **2** at an isosurface level of −30 e Å^{-5} and at C1 (bottom left) and C24 (bottom right) atoms at an isosurface level of −15 e Å^{-5}.

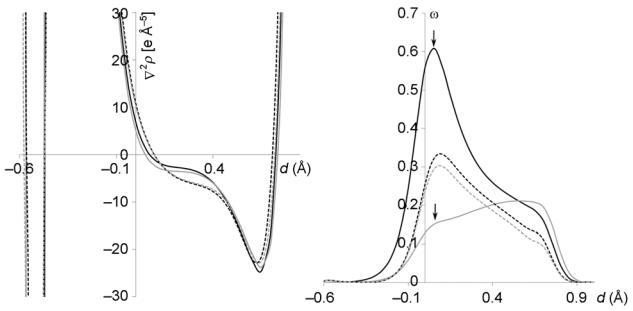

Figure 4. $\nabla^2\rho$ (*r*) along the Si1−C1 (black) and Si1−C24 (gray) bond paths (left). Ellipticity (∈) along the Si1−C1 (black) and Si1−C24 (gray) bond (right). Values of the experimental analysis are shown as solid lines; values of the theoretical analysis are shown as dashed lines.

electron density at the heteroatoms couples to the donating carbon atoms and the charge distribution at the carbon atoms mirrors predominantly that of a singlet carbene, substantiated by X-band EPR experiments.[11a]

The Laplacians along the Si1−C1 and Si1−C24 bond paths feature a very similar shape. At the BCP they have a slightly positive value and reach their minimum at about −30 e Å^{-5}, close to the carbene carbon atoms (Figure 4). The rather low ED at the BCP and the charge concentration and depletion along the different directions at the Si1−C1 and Si1−C24 BCPs support the very polar character of both Si−C bonds. In both cases η is less than unity and even smaller than in other previously reported cases for various analyzed Si−C, Si−O, Si−N,[21,14c] and S−N bonds[22] (Table 2). From this data, both Si−C bonds have to be regarded as very polar bonds with a slight covalent contribution. However, by analyzing the ellipticity ∈ along the bond paths, a significant difference in the Si1−C1 and Si1−C24 bonds is recognized, possibly indicating different π-contributions (Figure 4).

As shown by Scherer et al.,[21a] a shoulder in the gradient of ε close to the BCP can be related to a pronounced degree of π-contribution in the bonding. This is the case for both bonds. In the Si1−C1 bond, the maximum close to the BCP is even higher than the ellipticity close to the carbon atom. The Si1−C1 profile resembles almost perfectly that calculated for the model compound $H_2Si{=}CH_2$, while Si1−C24 shows admixing of $[H_3Si{-}CH_2]^-$ bonding.

The differences between the two bonds are also apparent in their other properties. There are small but significant differences in the bond lengths of Si1−C1 (1.8454(2) Å [1.824 Å]) and Si1−C24 (1.8615(2) Å [1.839 Å]), in the torsion angle between the five-membered ring and the silicon (C5-N1-C1-Si1 18.7(1)°[18.2°], C28-N2-C24-Si1 11.5(1)° [12.2]) in $\rho(r_{BCP})$ of 0.726 [0.742] for the Si1−C1 and 0.741 [0.762] e Å^{-3} for the Si1−C24 bond and the Bader charges of −0.51 [−0.31] for C1 and −0.37 [−0.26] e for C24 (Table 2 and Figure 5). Differences in the bond lengths and in the torsion angles were also reported for a similar germylone.[23] However, compounds with dimethyl groups instead of the cyclohexyl group do not show significant differences in these values, both in the silylone and the germylone.[23,12] Thus this might be attributed to packing effects. To elucidate them, we carried out periodic solid-state calculations. As shown recently by Mata et al.,[24] these calculations are vital to model weak intermolecular structure determining factors. By calculating increasing spheres of surrounding point charges representing the crystal packing, they were able to recover the changes in the properties of the charge density distribution caused by weak intermolecular interactions. However, modeling the crystal packing for such a big molecule as the present silylone is ambitious and almost inevitably leads to differences between the values obtained from experimental data. Nevertheless, the calculated values gained from the periodic solid-state calculation show the same trends as

Table 1: ED and Laplacian at the N−C BCPs.

	N1−C1	N1−C4	N1−C5	N2−C24	N2−C27	N2−C28
ρ [e Å^{-3}]	1.981	1.682	1.794	1.986	1.643	1.815
$\nabla^2\rho$ [e Å^{-5}]	−13.156	−10.602	−10.520	−13.287	−12.004	−12.003
∈	0.16	0.05	0.03	0.13	0.08	0.04

Table 2: Properties at the Si−C BCPs. Calculated values are given in squared brackets.

Bond	$\rho(r_{BCP})$ [e Å^{-3}]	$\nabla^2\rho(r_{BCP})$ [e Å^{-5}]	d_{BP} [Å]	$d1_{BP}$ [Å]	$d2_{BP}$ [Å]	λ_1	λ_2	λ_3	∈	η
Si1–C1	0.726	6.901	1.8460	0.7256	1.1203	−4.09	−2.62	13.62	0.56	0.30
	[0.742]	[10.838]				[−3.69]	[−2.87]	[17.47]	[0.29]	[0.21]
Si1–C24	0.741	5.095	1.8629	0.7292	1.1336	−3.95	−3.50	12.54	0.13	0.31
	[0.762]	[10.301]				[−3.55]	[−2.94]	[16.72]	[0.21]	[0.21]

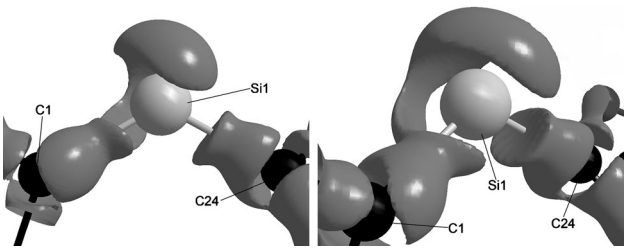

Figure 5. Laplacian distribution at Si1 from different directions at an isosurface level of $-1\ e\text{Å}^{-5}$.

the experimental values (Table 2). A QTAIM analysis of a calculated electron density distribution of the fixed experimental geometry is given in the Supporting Information.

In conclusion, we have shown by an experimental and theoretical charge density study that the interpretation of **2** as a silylone is valid. We were able to find two separated VSCCs present in the non-bonding region of the central silicon atom. The nitrogen–carbene-carbon bond seems to have a significant double bond character, indicating a singlet state for the carbene carbon, which is needed for donor–acceptor bonding. Thus the sum of bond angles at the nitrogen atoms seems to be a reasonable estimate for singlet versus triplet state of cAACs. The Bader charges correlate well with the values expected from NBO analysis.[11a] Furthermore, we were able to show that there are significant differences in the bonding situation of the two silicon carbon bonds, indicating a different amount of π-contribution. From periodic solid-state calculations, we were able to show that this is due to the different geometry of the two cAACs caused by weak intermolecular interactions.

Experimental Section

A high-resolution dataset of **2** was collected on a Bruker Smart APEX II Ultra with D8 three-circle goniometer, equipped with an APEX II CCD and a TXS Mo rotating anode and Incoatec Helios mirror optics. The single crystal was mounted from inert oil at low temperature and under nitrogen atmosphere using the X-Temp2 device.[25] Crystal data for **2**: $C_{46}H_{70}N_2Si{\cdot}0.5(C_6H_{14})$, $M=722.21\ g\,mol^{-1}$, triclinic space group $P\bar{1}$, $a=9.303(7)$, $b=12.054(8)$, $c=19.881(2)$ Å, $\alpha=95.53(3)$, $\beta=98.26(3)$, $\gamma=97.27(3)°$, $V=173.6(3)$ Å^3, $Z=2$, $2\Theta_{max.}=104.4°$, completeness = 98%, $\rho_{calcd}=1.107\ Mg\,m^{-3}$, $\mu=0.089\ mm^{-1}$, 663790 reflections measured, 49177 unique, $R1(I>1\sigma(I))=0.0249$, $wR2(I>1\sigma(I))=0.0452$, GoF = 2.6984 wGoF = 0.9930 after multipole refinement.

The structure was solved by direct methods (SHELXT-2013).[26] An IAM was refined with SHELXL-2013.[26] The multipole refinement with XD2006[27] was carried out against F^2 with a sigma cutoff of 1 (see the Supporting Information) using 10 resolution dependent scale factors. Some of the atoms showed anharmonic motion.[28] and were refined using the Gram–Charlier coefficients up to third order. Anisotropic displacement parameters for the hydrogen atoms were calculated with SHADE[29] using a riding model with neutron diffraction standard bond distances to the carbon atoms. The weighting scheme was chosen using normal probability plots.[30] XD2006[27] was used for the multipole refinement. CCDC-962955 (**2**) contains the supplementary crystallographic data for this paper. These data can be obtained free of charge from The Cambridge Crystallographic Data Centre via www.ccdc.cam.ac.uk/data_request/cif.

We optimized the system with periodic boundary conditions using the X-ray structure and the VASP program package in the version 5.2.12.[31] For the calculations, the PBE functional[32] together with the projector-augmented wave method (PAW)[33] was used. The cutoff value for the kinetic energy of the plane-wave basis set was set to 350 eV. The Brillouin zone was sampled by a G-centered *k*-point mesh generated by the Monkhorst–Pack method using a $3\times3\times3$ *k* mesh. The structure gained through this optimization was used to generate a wfx file with the Gaussian09 (Rev C.01) program package[34] at the BP86/def2-TZVPP level of theory. The same method was used to generate a wfx file of the X-ray structure by a single-point calculation. The wfx files were used together with the program AIMAll[35] to perform a QTAIM analysis.[16]

Received: October 2, 2013
Revised: October 31, 2013
Published online: January 30, 2014

Keywords: electron density · low oxidation states · silicon · sylylones

[1] a) N. Takagi, T. Shimizu, G. Frenking, *Chem. Eur. J.* **2009**, *15*, 8593 – 8604; b) N. Takagi, T. Shimizu, G. Frenking, *Chem. Eur. J.* **2009**, *15*, 3448 – 3456.

[2] R. Tonner, F. Öxler, B. Neumüller, W. Petz, G. Frenking, *Angew. Chem.* **2006**, *118*, 8206 – 8211; *Angew. Chem. Int. Ed.* **2006**, *45*, 8038 – 8042.

[3] a) R. Tonner, G. Frenking, *Angew. Chem.* **2007**, *119*, 8850 – 8853; *Angew. Chem. Int. Ed.* **2007**, *46*, 8695 – 8698; b) R. Tonner, G. Frenking, *Chem. Eur. J.* **2008**, *14*, 3260 – 3272; c) R. Tonner, G. Frenking, *Chem. Eur. J.* **2008**, *14*, 3273 – 3289; d) R. Tonner, G. Heydenrych, G. Frenking, *ChemPhysChem* **2008**, *9*, 1474 – 1481; e) G. Frenking, R. Tonner, *Pure Appl. Chem.* **2009**, *81*, 597 – 614; f) N. Takagi, R. Tonner, G. Frenking, *Chem. Eur. J.* **2012**, *18*, 1772 – 1780.

[4] C. A. Dyker, V. Lavallo, B. Donnadieu, G. Bertrand, *Angew. Chem.* **2008**, *120*, 3250 – 3253; *Angew. Chem. Int. Ed.* **2008**, *47*, 3206 – 3209.

[5] M. Alcarazo, C. W. Lehmann, A. Anoop, W. Thiel, A. Fürstner, *Nat. Chem.* **2009**, *1*, 295 – 301.

[6] a) M. Christl, B. Engels, *Angew. Chem.* **2009**, *121*, 1566 – 1567; *Angew. Chem. Int. Ed.* **2009**, *48*, 1538 – 1539; b) M. M. Hänninen, A. Peuronen, H. M. Tuononen, *Chem. Eur. J.* **2009**, *15*, 7287 – 7291; c) V. Lavallo, C. A. Dyker, B. Donnadieu, G. Bertrand, *Angew. Chem.* **2009**, *121*, 1568 – 1570; *Angew. Chem. Int. Ed.* **2009**, *48*, 1540 – 1542; d) D. S. Patel, P. V. Bharatam, *J. Org. Chem.* **2011**, *76*, 2558 – 2567; e) A. Guha, B. Konwar, S. Sarmah, A. Phukan, *Theor. Chem. Acc.* **2012**, *131*, 1 – 11.

[7] a) S. Ishida, T. Iwamoto, C. Kabuto, M. Kira, *Nature* **2003**, *421*, 725 – 727; b) M. Kira, T. Iwamoto, S. Ishida, H. Masuda, T. Abe, C. Kabuto, *J. Am. Chem. Soc.* **2009**, *131*, 17135 – 17144.

[8] H. Tanaka, S. Inoue, M. Ichinohe, M. Driess, A. Sekiguchi, *Organometallics* **2011**, *30*, 3475 – 3478.

[9] a) M. Kosa, M. Karni, Y. Apeloig, *J. Am. Chem. Soc.* **2004**, *126*, 10544 – 10545; b) M. Kosa, M. Karni, Y. Apeloig, *J. Chem. Theory Comput.* **2006**, *2*, 956 – 964; c) T. Veszprémi, K. Petrov, C. T. Nguyen, *Organometallics* **2006**, *25*, 1480 – 1484.

[10] a) V. Lavallo, Y. Canac, A. DeHope, B. Donnadieu, G. Bertrand, *Angew. Chem.* **2005**, *117*, 7402 – 7405; *Angew. Chem. Int. Ed.* **2005**, *44*, 7236 – 7239; b) V. Lavallo, Y. Canac, C. Präsang, B. Donnadieu, G. Bertrand, *Angew. Chem.* **2005**, *117*, 5851 – 5855; *Angew. Chem. Int. Ed.* **2005**, *44*, 5705 – 5709; c) M. Melaimi, M. Soleilhavoup, G. Bertrand, *Angew. Chem.* **2010**, *122*, 8992 – 9032; *Angew. Chem. Int. Ed.* **2010**, *49*, 8810 – 8849; d) D. Martin, M. Soleilhavoup, G. Bertrand, *Chem. Sci.* **2011**, *2*, 389 – 399.

[11] a) K. C. Mondal, H. W. Roesky, M. C. Schwarzer, G. Frenking, B. Niepötter, H. Wolf, R. Herbst-Irmer, D. Stalke, *Angew. Chem.* **2013**, *125*, 3036 – 3040; *Angew. Chem. Int. Ed.* **2013**, *52*, 2963 – 2967; b) K. C. Mondal, H. W. Roesky, M. C. Schwarzer, G. Frenking, I. Tkach, H. Wolf, D. Kratzert, R. Herbst-Irmer, B. Niepötter, D. Stalke, *Angew. Chem.* **2013**, *125*, 1845 – 1850; *Angew. Chem. Int. Ed.* **2013**, *52*, 1801 – 1805.
[12] K. C. Mondal, P. P. Samuel, M. Tretiakov, A. P. Singh, H. W. Roesky, A. C. Stückl, B. Niepötter, E. Carl, H. Wolf, R. Herbst-Irmer, D. Stalke, *Inorg. Chem.* **2013**, *52*, 4736 – 4743.
[13] Y. Xiong, S. Yao, S. Inoue, J. D. Epping, M. Driess, *Angew. Chem.* **2013**, *125*, 7287 – 7291; *Angew. Chem. Int. Ed.* **2013**, *52*, 7147 – 7150.
[14] a) R. S. Ghadwal, H. W. Roesky, S. Merkel, J. Henn, D. Stalke, *Angew. Chem.* **2009**, *121*, 5793 – 5796; *Angew. Chem. Int. Ed.* **2009**, *48*, 5683 – 5686; b) A. Jana, D. Leusser, I. Objartel, H. W. Roesky, D. Stalke, *Dalton Trans.* **2011**, *40*, 5458 – 5463; c) D. Kratzert, D. Leusser, J. J. Holstein, B. Dittrich, K. Abersfelder, D. Scheschkewitz, D. Stalke, *Angew. Chem.* **2013**, *125*, 4574 – 4578; *Angew. Chem. Int. Ed.* **2013**, *52*, 4478 – 4482.
[15] N. K. Hansen, P. Coppens, *Acta Crystallogr. Sect. A* **1978**, *34*, 909 – 921.
[16] R. F. W. Bader, *Atoms in Molecules—A Quantum Theory*, Oxford University Press, New York, **1990**.
[17] J. Hey, D. Leusser, D. Kratzert, H. Fliegl, R. A. Mata, J. M. Dieterich, D. Stalke, *Phys. Chem. Chem. Phys.* **2013**, *15*, 20600 – 20610.
[18] The calculations gave one VSCC in the non-bonding region of Si with similar values to the experimental data. The calculated second VSCC is located much closer to the nucleus and has a much larger negative value for the Lapacian $\nabla^2\rho\,(r)$. We think that this is a numerical artefact of the method.
[19] R. F. W. Bader, R. J. Gillespie, P. J. MacDougall, *J. Am. Chem. Soc.* **1988**, *110*, 7329 – 7336.
[20] M. Tafipolsky, W. Scherer, K. Öfele, G. Artus, B. Pedersen, W. A. Herrmann, G. S. McGrady, *J. Am. Chem. Soc.* **2002**, *124*, 5865 – 5880.
[21] a) W. Scherer, P. Sirsch, D. Shorokhov, G. S. McGrady, S. A. Mason, M. G. Gardiner, *Chem. Eur. J.* **2002**, *8*, 2324 – 2334; b) G. V. Gibbs, A. E. Whitten, M. A. Spackman, M. Stimpfl, R. T. Downs, M. D. Carducci, *J. Phys. Chem. B* **2003**, *107*, 12996 – 13006; c) N. Kocher, C. Selinka, D. Leusser, D. Kost, I. Kalikhman, D. Stalke, *Z. Anorg. Allg. Chem.* **2004**, *630*, 1777 – 1793; d) Y. Yang, *J. Phys. Chem. A* **2010**, *114*, 13257 – 13267.
[22] a) D. Leusser, J. Henn, N. Kocher, B. Engels, D. Stalke, *J. Am. Chem. Soc.* **2004**, *126*, 1781 – 1793; b) J. Henn, D. Leusser, D. Ilge, D. Stalke, B. Engels, *J. Phys. Chem. A* **2008**, *112*, 9442 – 9452.
[23] Y. Li, K. C. Mondal, H. W. Roesky, H. Zhu, P. Stollberg, R. Herbst-Irmer, D. Stalke, D. M. Andrada, *J. Am. Chem. Soc.* **2013**, *135*, 12422 – 12428.
[24] J. Hey, D. M. Andrada, R. Michel, R. A. Mata, D. Stalke, *Angew. Chem.* **2013**, *125*, 10555 – 10559; *Angew. Chem. Int. Ed.* **2013**, *52*, 10365 – 10369.
[25] a) T. Kottke, D. Stalke, *J. Appl. Crystallogr.* **1993**, *26*, 615 – 619; b) D. Stalke, *Chem. Soc. Rev.* **1998**, *27*, 171 – 178.
[26] G. M. Sheldrick, *Acta Crystallogr. Sect. A* **2008**, *64*, 112 – 122.
[27] A. Volkov, P. Macchi, L. J. Farrugia, C. Gatti, P. R. Mallinson, T. Richter, T. Koritsanszky, XD2006, **2006**.
[28] a) K. Meindl, R. Herbst-Irmer, J. Henn, *Acta Crystallogr. Sect. A* **2010**, *66*, 362 – 371; b) R. Herbst-Irmer, J. Henn, J. J. Holstein, C. B. Hübschle, B. Dittrich, D. Stern, D. Kratzert, D. Stalke, *J. Phys. Chem. A* **2013**, *117*, 633 – 641.
[29] A. Ø. Madsen, *J. Appl. Crystallogr.* **2006**, *39*, 757 – 758.
[30] V. V. Zhurov, E. A. Zhurova, A. A. Pinkerton, *J. Appl. Crystallogr.* **2008**, *41*, 340 – 349.
[31] a) G. Kresse, J. Furthmüller, *J. Comput. Math. Sci.* **1996**, *6*, 15 – 50; b) G. Kresse, J. Furthmüller, *Phys. Rev. B* **1996**, *54*, 11169 – 11186.
[32] a) J. P. Perdew, K. Burke, M. Ernzerhof, *Phys. Rev. Lett.* **1996**, *77*, 3865 – 3868; b) J. P. Perdew, K. Burke, M. Ernzerhof, *Phys. Rev. Lett.* **1997**, *78*, 1396.
[33] a) P. E. Blöchl, *Phys. Rev. B* **1994**, *50*, 17953 – 17979; b) G. Kresse, D. Joubert, *Phys. Rev. B* **1999**, *59*, 1758 – 1775.
[34] Gaussian 09, Revision C.01, M. J. Frisch, et al., Gaussian, Inc., Wallingford CT, **2010**.
[35] T. Keith, AIMAll (Version 13.05.06), TK Gristmill Software, Overland Park KS, **2013**.

